

The Influence of Local Phonon Modes in a Wide-Band Matrix on the Tunnel Current-Voltage Characteristics of Quasi-Zero-Dimensional Structures

V. Ch. Zhukovsky^{a*}, V. D. Krevchik^{b***}, M. B. Semenov^b, R. V. Zaytsev^b,
D. O. Filatov^{c****}, P. V. Krevchik^b, and A. A. Bukharaev^{d*****}

^a Department of Physics, Moscow State University, Moscow, 119991 Russia

^b Department of Physics, Penza State University, Penza, 440026 Russia

^c Lobachevsky University of Nizhni Novgorod, Nizhni Novgorod, 603950 Russia

^d Zavoisky Institute for Physics and Technology, Kazan Scientific Center, Russian Academy of Sciences,
Kazan, 420029 Russia

^e Volga Region Federal University, Kazan, 420000 Russia

*e-mail: vlchzh@gmail.com;

**e-mail: physics@pnzgu.ru;

***e-mail: dmitry_filatov@inbox.ru;

****e-mail: Bukharaev@kfii.knc.ru

Received March 17, 2014; in final form, April 19, 2014

Abstract—Experimental results on the visualization of the density of states in InAs/GaSb(001) quantum dots that were obtained by tunnel atomic-force microscopy in an ultrahigh vacuum are presented. A one-dimensional (1D) model of dissipative quantum tunneling is proposed for describing experimental current-voltage characteristics of a tunnel contact between an atomic force microscope probe and the surface of InAs/GaSb(001) quantum dots. It was found that the influence of two local modes of the wide-band matrix on the probability of 1D dissipative tunneling leads to the appearance of several randomly spaced peaks in the field dependence. It was shown that the theoretical dependence agrees qualitatively with experimental the current-voltage characteristic of the atomic force microscope tip and the surface of InAs/GaSb(001) quantum dots.

Keywords: quantum tunneling with dissipation, quantum dots, tunnel current-voltage characteristics.

DOI: 10.3103/S0027134914040110

INTRODUCTION

Methods of scanning-probe microscopy, including scanning tunneling microscopy (STM) and atomic force microscopy (AFM) are widely used in studying morphology, atomic structure and energy spectrum of semiconductor quantum-dimensional structures [1–22]. The STM method of transverse cleavages in an ultrahigh vacuum (UHV) was applied for measuring the local density of states (LDS) in quantum wells (see, for example, [10]). The present work was initiated by an experiment that was performed at Zavoisky Institute for Physics and Technology, Kazan Scientific Center of the Russian Academy of Sciences and devoted to the measurements of tunnel current–voltage characteristics (CVCs) in semiconductor InAs/GaSb(001) quantum dots (QDs). In these experiments, several non-equidistant peaks were discovered, which we explained in the framework of the model of 1D-dissipative tunneling with allowance for one local phonon mode [11]. The proposed theoretical model allowed us to reveal only two single peaks,

one of which is unstable, which is not quite in agreement with the experimental data. It is worth noting that the features on the observed tunnel CVCs are usually interpreted in the model of resonance tunneling (see, for example, [1, 5, 7–9]). In this paper a hypothesis on the possibility of a tunnel transport mechanism with the participation of two promoting phonon modes of the wide-band matrix is proposed and substantiated theoretically. The non-resonance mechanism of tunnel transport, which is characteristic for metal QD, may occur in the doped QD under the condition when the concentration of charge carriers can be varied using an external electric field in a rather broad limits.

This work has the following aims:

- i) Experimental study of tunnel CVCs obtained upon the visualization of the local density of states in InAs/GaSb(001) quantum dots using AFM microscopy;
- ii) The theoretical study of oscillating and non-oscillating modes of 1D-dissipative tunnel transport

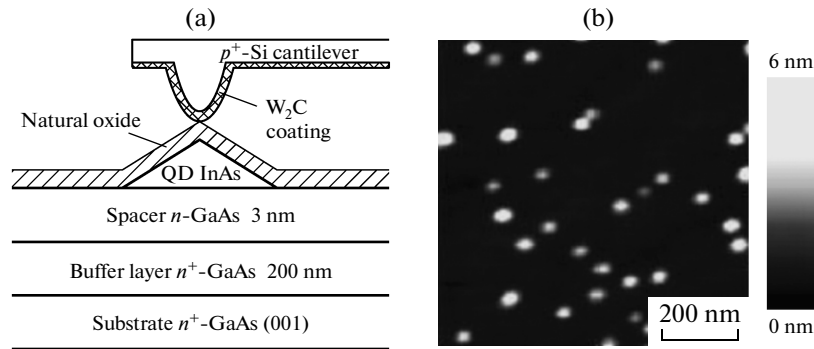


Fig. 1. The scheme of the current imaging mode of the surface of InAs/GaAs(001) QDs; an AFM image of InAs/GaAs(001) QDs (b).

with allowance for two local phonon modes of the broad-band matrix in an external electric field at a finite temperature.

We carried out a qualitative comparison of the theoretical dependence for the probability of 1D-tunneling from the strength of an external electric field with experimental CVCs for the contact of an atomic force microscope tip and the surface of a QD.

MATERIALS AND METHODS

The specimens for the tunnel AFM investigation of spatial and energy LDS distributions in the quantum dots InAs were grown by B.N. Zvonkov on the substrates of n -GaAs (001) doped by Si (AGCHO brand) using MOS-hydride epitaxy at atmospheric pressure (Research Institute of Physics and Technology, Lobachevsky University of Nizhni Novgorod). Figure 1a shows the scheme of the specimens. Buffer Si-doped n -GaAs layers with a thickness of 200 nm and the donor concentration $N_D \sim 10^{18} \text{ cm}^{-3}$ were grown at a temperature of 650°C . The spacer layers of non-doped n -GaAs ($N_D \sim 10^{15} \text{ cm}^{-3}$) with a thickness of ≈ 3 nm needed to form the triangle potential barrier between QD and the n^+ -GaAs buffer layer were grown on the top of specimens [25]. GaAs QD were formed by the Stranski–Krastanov mechanism at a temperature of 530°C . The nominal thickness of the deposited InAs layer is ≈ 1.5 nm.

The experiment on the visualization of spatial LDS distribution in InAs/GaAs(001) QDs was performed at the Zavoisky Institute for Physics and Technology of the Kazan Scientific Center of the Russian Academy of Sciences. We used an Omicron UHV AFM/STM VT scanning-probe microscope (SPM) at a high vacuum at room temperature, which is a part of the UHV Omicron MultiProbe P. The base pressure in the SPM chamber was $\sim 10^{-10}$ Torr. The surface of the sample, which was covered by natural oxide and formed during the process of transportation of the setup for growing into the UHV chamber for the SPM studies, was

scanned by means of a W_2C -covered p^+ -Si AFM probe in the contact mode (Fig. 1a). Moreover, the bias voltage, V_g , was fed between the n^+ -GaAs sample and the AFM tip. The spatial distributions of the current I , between the tip and the sample depending on the probe x, y coordinates in the plane of the sample were recorded at the constant value $V_g = \text{const}$ (images of current). The CVCs in the contact of an AFM tip and the surface of a QD were obtained by means of a series of images of current at various values of V_g . The methodology for growing and QD tunnel spectroscopy has been described in detail [23].

Figure 1b shows an AFM image of the sample surface. Surface QDs have a height $h = 5\text{--}6$ nm. It must be noted that lateral dimensions of QDs (Fig. 1b) considerably exceed the expected values of a QD and have the form of a four-sided pyramid faceted by (101) planes for these values of height h (10–12 nm). This is caused by the convolution effect due to the finite dimensions of the curvature radius of the AFM probes $R_p \approx 35$ nm [25].

On the tunnel spectra of QDs (Fig. 2), the peaks were found related to the electron tunneling from the filled electron states beneath the Fermi level in the material of the W_2C coating of the AFM probe to the levels of dimensional quantization in QDs [11, 23]. When interpreting tunnel spectra in QDs one should take into account the fact that the experiments were carried out at room temperature and correspondingly the processes of electron tunneling accompanied by the emission/absorption of phonons are possible under these conditions. Earlier this factor was not taken into consideration when interpreting the tunnel spectra of InAs/GaAs(001) QDs [11, 23].

A qualitative comparison of the theoretical probability curve for the 1D-dissipative tunneling (with allowance for one local phonon mode in a semiconductor matrix) and experimental CVCs for InAs/GaAs(001) QDs is shown in Fig. 2. As we can see, only two non-equidistant peaks on the experimental CVCs agree qualitatively with the theoretical

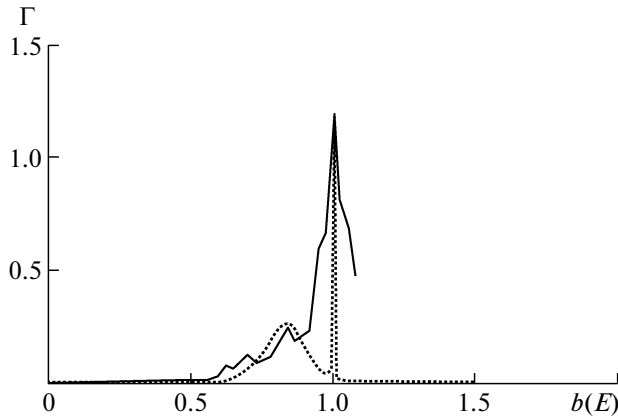


Fig. 2. The theoretical curve with allowance for a local mode of dielectric matrix (dashed line) and the experimental curve (solid line) [11].

peaks, one of which is unstable in the considered model. This result necessitates the refinement of a theoretical model for an adequate description of the experimental data of the tunnel QD spectroscopy. At the same time, two types of optical phonons are known to exist in GaAs: transverse (TO) phonons with the energy $\hbar\Omega = 34$ meV and longitudinal (LO) phonons with the energy $\hbar\Omega = 38$ meV [25]. In this relationship, the analysis of two local phonon modes of the wide-band matrix in weak dissipation mode is expedient.

CALCULATION OF THE PROBABILITY OF 1D-DISSIPATIVE TUNNELING WITH ACCOUNT FOR TWO LOCAL PHONON MODES OF THE WIDE-BAND MATRIX

Qualitative comparison of the theoretical probabilistic curve of the 1D-dissipative tunneling (with allowance for a single local phonon mode of the dielectric matrix) and experimental CVCs for semiconductor InAs/GaAs(001) QDs is shown in Fig. 2. As we can see, only two non-equidistant peaks in the series on experimental CVCs agree qualitatively with theoretical calculations; however, one of them proved to be unstable in this model. This result required a clarification of the theoretical model with allowance for two local modes of the wide-band matrix in weak dissipation regime.

The problem statement is analogous to that used by the authors previously when analyzing the 1D-dissipative model of tunneling with an instanton-like oscillator potential in an external electric field (Fig. 3) at a finite temperature. Moreover, the standard dissipative tunnel Hamiltonian with allowance for two phonon modes of the wide-band matrix is used [12]. The units $\hbar = m = 1$ are used in what follows.

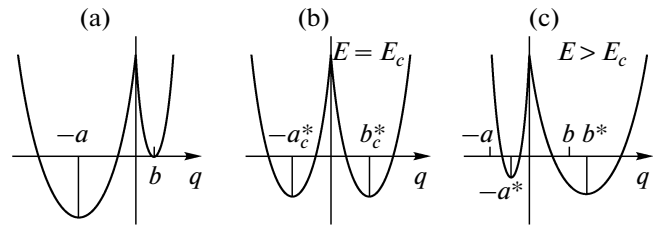


Fig. 3. The impact of the electric field on the asymmetrical instanton potential. Figure 1b shows the case of the symmetrical potential at a definite value of the electric field strength.

One can show that the 1D-quasiclassical action in single-instanton approximation with allowance for the effect of the wide-band matrix takes the form

$$S_B = 2\omega_0^2(q_0 + q_1)q_0\tau_0 - \frac{2\omega_0^2(q_0 + q_1)^2\tau_0^2}{\beta} - \frac{4\omega_0^4(q_0 + q_1)^2}{\beta} \sum_{n=1}^{\infty} \frac{\sin^2 v_n \tau_0}{(v_n^2 + \omega_0^2 + \zeta_n)}, \quad (1)$$

where q_1 and q_0 are the parameters of renormalized instanton-like oscillator potential in an external magnetic field $q_1 = b = b^* + \frac{|e|E}{\omega_0^2}$, $q_0 = a = a^* - \frac{|e|E}{\omega_0^2}$. The

external electric field applied along the tunnel coordinate changes the symmetry of the 1D-oscillator potential, as shown in Fig. 3. The exponential prefactor is determined by the contribution of trajectories located close to the instanton. For this purpose, the action must be expanded in a series up to quadratic term in $q - q_B$ and then integrated in the functional space. Then the probability of tunneling per unit time is given by

$$\Gamma = B \exp(-S_B),$$

where the exponential prefactor B has the form [12]

$$B = \left[\frac{S_0}{2\pi} \frac{\det' \left(\frac{\delta^2 S}{\delta q^2} \right)_{q=-q_0}}{\det' \left(\frac{\delta^2 S}{\delta q^2} \right)_{q=q_B(\tau)}} \right]^{1/2},$$

$$S_0 = \int_{-\beta/2}^{\beta/2} \dot{q}_B^2(\tau) d\tau.$$

Here \det' implies that the zero eigen value corresponding to the zero instanton mode is omitted. It should be noted that the derivation of this formula needs the condition of an ideal instanton gas

$$\Gamma \ll (\Delta\tau)^{-1},$$

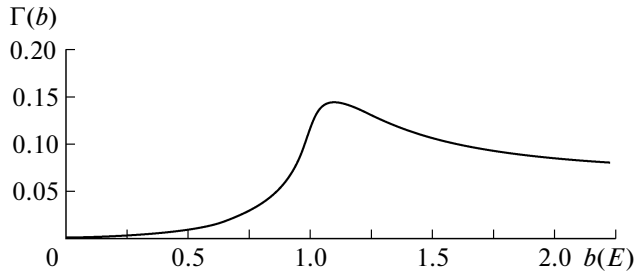


Fig. 4. The theoretical dependence of the probability of dissipative tunneling in the non-oscillating current-transport mode.

where $\Delta\tau$ is the width of the transition from the positive value of trajectory to the negative one. The calculated preexponential factor in this model is given by

$$B = \frac{2\omega_0^2(q_0 + q_1)^2}{(2\pi\beta)^{1/2}} \sum_{n=-\infty}^{\infty} \frac{\sin^2 v_n \tau_0 \left(\frac{\cos 2v_n \tau_0}{\lambda_{0n}}\right)^{-1/2}}{\lambda_{0n}},$$

where v_n are the Matsubara frequencies, β is the inverse temperature, and τ_0 is the center of instanton.

Consider (1) with allowance for two local modes ($\omega_{L1} = \omega_2$ and $\omega_{L2} = \omega_3$). To simplify the problem, we assume that this interaction is relatively small, i.e., $\frac{C_\alpha}{\omega_0^2} \ll 1$ and $\frac{C_\alpha}{\omega_L^2} \ll 1$. In this case $\zeta_n =$

$$v_n^2 \sum_{\alpha=2}^N \frac{C_\alpha^2}{(\omega_\alpha^2 + v_n^2)}, \text{ where } v_n = \frac{2\pi n}{\beta}, \beta = \frac{\hbar}{kT}, C_\alpha \text{ are}$$

the coefficients of interaction of a tunnel particle with the local phonon modes of dielectric matrix,

$$\zeta_n = v_n^2 \frac{C_2^2}{\omega_2^2(\omega_2^2 + v_n^2)} + v_n^2 \frac{C_3^2}{\omega_3^2(\omega_3^2 + v_n^2)}.$$

The expression for the 1D-probability of dissipative tunneling with an accuracy to the preexponential factor is given in the Appendix.

The obtained analytical formula for the probability of 1D dissipative tunneling with allowance for two local phonon modes of dielectric matrix makes it possible to study the features of the $\Gamma(E)$ dependence. This is important for comparison with the experimental tunnel CVCs. In addition, theoretical results have shown that the dependence of the probability of 1D-dissipative tunneling on the external electric field strength at a finite temperature and fixed parameters of the dielectric matrix describes both oscillating and nonoscillating tunneling regimes (Figs. 4, 5).

Figure 5 shows a qualitative comparison of the theoretical dependence for the probability of 1D dissipative tunneling on the external electric field (with allowance for two phonon modes) and an experimen-

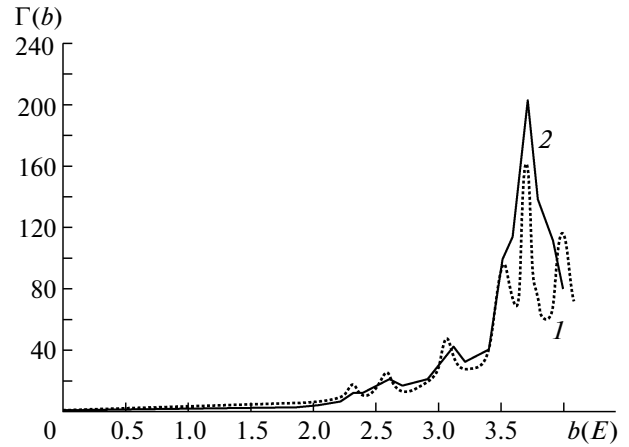


Fig. 5. The theoretical probability of dissipative tunneling in an oscillating regime with allowance for two local phonon modes (curve (1)) and the experimental curve (2).

tal CVCs for InAs/GaAs(001) QDs. From Fig. 5 we can see that the characteristic non-equidistant spectrum of peaks on experimental CVCs shows a better qualitative agreement with the peaks of the theoretical dependence for the probability of 1D dissipative tunneling than in the case of the model that takes a single local phonon mode of the wide-band matrix into account [11].

CONCLUSIONS

We calculated the probability for the 1D dissipative tunneling in an instanton-like oscillator potential with allowance for two promoting local phonon modes of the wide-band matrix at a finite temperature upon the action of an external electric field. The mode of oscillating tunnel transport in the limit of weak dissipation and the non-oscillating mode were considered. A dissipative tunneling mode in the limit of weak dissipation is likely characteristic in degenerate semiconductors together with common resonance tunneling mode. The oscillation regime of dissipative tunneling made it possible to reveal the qualitative agreement with known experimental data theoretically. When interpreting the tunnel spectra of QDs in an experimental investigation, the processes of electron tunneling with phonon emission and absorption were assumed to occur. It is worth noting that this fact was not taken into consideration previously [11, 23] when interpreting tunnel spectra in InAs/GaAs(001) QDs.

Therefore, together with the resonance tunneling regime [1, 8, 9], as previously assumed, it is also necessary to consider the contribution from the dissipative oscillating regime (in the limit of weak dissipation),

which may be observed on the tunnel CVCs of a semiconductor QD placed in a wide-band matrix.

ACKNOWLEDGMENTS

The authors are thankful to B.N. Zvonkov for his assistance in growing crystals and P.A. Borodin for performing the experiments.

APPENDIX

The derivation is given here of the formula for the probability of 1D-dissipative tunneling with an accuracy to the preexponential factor. In the case of two promoting phonon modes, the quasiclassical action (1) is reduced to a sum of two kinds in the last term

$$U_1 = \frac{1}{2} \sum_{n=1}^{\infty} \frac{1}{v_n^2 \left(v_n^2 + \omega_0^2 + v_n^2 \frac{C_2^2}{\omega_2^2(\omega_2^2 + v_n^2)} v_n^2 + \frac{C_3^2}{\omega_3^2(\omega_3^2 + v_n^2)} \right)},$$

$$U_2 = \frac{1}{2} \sum_{n=1}^{\infty} \frac{\cos 2v_n \tau_0}{v_n^2 \left(v_n^2 + \omega_0^2 + v_n^2 \frac{C_2^2}{\omega_2^2(\omega_2^2 + v_n^2)} v_n^2 + \frac{C_3^2}{\omega_3^2(\omega_3^2 + v_n^2)} \right)}.$$
(A1)

Denoting $v_n^2 = x$ and $A = \omega_2^2 + \omega_3^2 + \omega_0^2 + \frac{C_2^2}{\omega_2^2} + \frac{C_3^2}{\omega_3^2}$,
 $B_\omega = \omega_2^2 \omega_3^2 + \omega_0^2(\omega_2^2 + \omega_3^2) + \frac{C_2^2 \omega_3^2}{\omega_2^2} + \frac{C_3^2 \omega_2^2}{\omega_3^2}$, $C = \omega_0^2 \omega_2^2 \omega_3^2$, the expression in the denominator of U_1 takes the form

$$x \omega_2^2 \omega_3^2 [x^3 + Ax^2 + B_\omega x + C]$$

$$= x \omega_2^2 \omega_3^2 (x - x_1)(x - x_2)(x - x_3).$$

We also denote

$$Q = \frac{A^2 - 3B_\omega}{9}; \quad R = \frac{2A^3 - 9AB_\omega + 27C}{54};$$

$$S = Q^3 - R^2; \quad \Phi = \frac{1}{3} \arccos\left(\frac{R}{\sqrt{Q^3}}\right).$$

If $S > 0$, then

$$x_1 = -2\sqrt{Q} \cos(\Phi) - \frac{A}{3},$$

$$x_2 = -2\sqrt{Q} \cos\left(\Phi + \frac{2}{3}\pi\right) - \frac{A}{3},$$

$$x_3 = -2\sqrt{Q} \cos\left(\Phi - \frac{2}{3}\pi\right) - \frac{A}{3},$$
(A2)

and the first sum in (P1) takes the form

$$U_1 = \frac{1}{2} \sum_{n=1}^{\infty} \frac{\omega_2^2 \omega_3^2 (\omega_2^2 + v_n^2)(\omega_3^2 + v_n^2)}{v_n^2 \omega_2^2 \omega_3^2 (v_n^2 - x_1)(v_n^2 - x_2)(v_n^2 - x_3)}. \quad (A3)$$

We decompose the last expression on simple fractions and denote

$$\frac{\beta_0}{x} + \frac{\gamma}{x - x_1} + \frac{\varphi}{x - x_2} + \frac{\Delta}{x - x_3}$$

$$= \frac{x^2 + x(\omega_2^2 + \omega_3^2) + \omega_2^2 \omega_3^2}{x(x - x_1)(x - x_2)(x - x_3)},$$

where

$$\beta_0 = -\frac{\omega_2^2 \omega_3^2}{x_1 x_2 x_3},$$

$$\Delta = \frac{x_3^2}{(x_3 - x_2)(x_1 - x_3)} \left\{ \frac{\omega_2^2 \omega_3^2}{x_1 x_2 x_3} \left(\frac{x_1 x_2 + x_1 x_3 + x_2 x_3}{x_2 x_3} - 1 \right) \right.$$

$$+ \frac{\omega_2^2 + \omega_3^2}{x_2 x_3} - \frac{1}{x_3} \left(1 + \frac{\omega_2^2 \omega_3^2}{x_1 x_2 x_3} \left[\frac{x_1 x_2 + x_1 x_3 + x_2 x_3}{x_2 x_3} \right. \right.$$

$$\left. \left. + (x_2 + x_3 - x_1) \right] \right) + \frac{(\omega_2^2 + \omega_3^2)(x_2 + x_3)}{x_2 x_3} \left. \right\}, \quad (A4)$$

$$\varphi = \frac{x_2}{x_3(x_2 - x_1)} \left\{ \Delta \frac{x_2}{x_3} (x_1 - x_3) - 1 - \frac{\omega_2^2 \omega_3^2}{x_1 x_2 x_3} (x_2 + x_3 - x_1) \right.$$

$$\left. - \frac{x_2 + x_3}{x_2 x_3} \left\{ \omega_2^2 + \omega_3^2 + \frac{\omega_2^2 \omega_3^2}{x_1 x_2 x_3} (x_1 x_2 + x_1 x_3 + x_2 x_3) \right\} \right\},$$

$$\gamma = \frac{1}{x_2 x_3} \{ \omega_2^2 + \omega_3^2 - \Delta x_1 x_2 - \varphi x_1 x_3$$

$$- \beta_0(x_2 x_3 + x_1(x_2 + x_3)) \}, \quad v_n = \frac{2\pi n}{\beta}.$$

As a result, U_1 is transformed to the form

$$U_1 = \frac{1}{2} \sum_{n=1}^{\infty} \left(\frac{\beta_0}{v_n^2} + \frac{\gamma}{v_n^2 - x_1} + \frac{\phi}{v_n^2 - x_2} + \frac{\Delta}{v_n^2 - x_3} \right).$$

$$x_1 = -2\sqrt{Q} \cos \phi - \frac{A}{3} = -x_{10} = -\left(2\sqrt{Q} \cos \phi + \frac{A}{3} \right);$$

$$x_2 = -2\sqrt{Q} \cos \left(\Phi + \frac{2}{3}\pi \right) - \frac{A}{3} = -x_{20} \quad \tilde{x}_{20}^2 = \frac{x_{20}\beta^2}{4\pi^2},$$

$$x_3 = -2\sqrt{Q} \cos \left(\Phi - \frac{2}{3}\pi \right) - \frac{A}{3} = -x_{30} \quad \tilde{x}_{30}^2 = \frac{x_{30}\beta^2}{4\pi^2}.$$

If $x_1 > 0, x_2 > 0, x_3 > 0$, then the quasiclassical action with allowance for two promoting modes reduces to the expression

$$S_B = 2\omega_0^2(a+b)a\tau_0 - \frac{2}{\beta}\omega_0^2(a+b)^2\tau_0^2 - \frac{4}{\beta}\omega_0^4(a+b)^2\{U_1 + U_2\},$$

where

$$\begin{aligned} \tau_0 &= \frac{1}{2\omega_0} \operatorname{arcsinh} \left[\frac{b-a}{b+a} \sinh \frac{\omega_0\beta}{4} \right] + \frac{\beta}{4} \\ &= \frac{1}{2\omega_0} \operatorname{arcsinh} \left[\frac{\frac{b-1}{a} \sinh \frac{\omega_0\beta}{4}}{\frac{b+1}{a}} \right] + \frac{\beta}{4} \end{aligned}$$

or

$$\begin{aligned} \tau_0^* &= \tau_0\omega_0 = \frac{1}{2} \operatorname{arcsinh} \left[\frac{b^*-1}{b^*+1} \sinh \beta^* \right] + \beta^*; \\ \tau_0^* &= \tau_0\omega_0; \quad \beta^* = \frac{\omega_0\beta}{4}. \end{aligned}$$

Finally, the renormalized expression for the 1D quasiclassical instanton action with allowance for two local modes of the dielectric matrix takes the form

$$\tilde{S}_B = \frac{S_B}{\omega_0 a^2} = 2(b^*+1)\tau_0^* - \frac{1}{2\beta^*}(b^*+1)^2\tau_0^{*2}$$

$$\begin{aligned} -\frac{(b^*+1)^2}{\beta^*} \left\{ \frac{1}{2} \left[\beta_0\omega_0^2 \left(\frac{\beta\omega_0}{4} \right)^2 \frac{2}{3} + 4 \frac{\gamma\omega_0^2 \left(\frac{\beta\omega_0}{4} \right)^2}{\pi^2} \left[-\frac{4\pi^2}{2x_1\beta^2} \right. \right. \right. \\ \left. \left. \left. - \frac{\pi^2}{\sqrt{x_1}\beta} \cot \left(\frac{\sqrt{x_1}\beta}{2\pi} \right) \right] + 4 \frac{\phi\omega_0^2\beta^{*2}}{\pi^2} \left[-\frac{4\pi^2}{2x_2\beta^2} \right. \right. \right. \end{aligned}$$

$$\left. \left. \left. - \frac{\pi^2}{\sqrt{x_2}\beta} \cot \left(\frac{\sqrt{x_2}\beta}{2\pi} \right) \right] + \frac{\Delta\omega_0^2\beta^{*2}}{\pi^2} \left[-\frac{4\pi^2}{2x_3\beta^2} \right. \right. \right.$$

$$\left. \left. \left. - \frac{\pi^2}{\sqrt{x_3}\beta} \cot \left(\frac{\sqrt{x_3}\beta}{2\pi} \right) \right] \right\} - \frac{1}{2} \left[\beta_0\omega_0^2 \left(\frac{\beta\omega_0}{4} \right)^2 \frac{1}{3} \left(3 \left(\frac{4\pi\tau_0\omega_0}{\beta\omega_0} \right)^2 \right. \right.$$

$$\left. \left. - \frac{6\pi^2\tau_0\omega_0^4}{\beta\omega_0} + 2\pi^2 \right) + \frac{4\gamma\omega_0^2 \left(\frac{\beta\omega_0}{4} \right)^2}{\pi^2} \right.$$

$$\left. \times \left\{ \frac{\omega_0\pi^2 4}{4\sqrt{x_1}\beta\omega_0} \cos \left[\left(\pi - \frac{4\pi\tau_0\omega_0}{\beta\omega_0} \right) \frac{\sqrt{x_1}2\beta\omega_0}{\omega_0\pi 4} \right] \right\} \right. \quad (A5)$$

$$\left. \times \operatorname{cosec} \frac{2\sqrt{x_1}\beta_0\omega_0}{\omega_0} + \frac{\omega_0\pi^2 4}{8x_1\beta\omega_0} \right\} + \frac{4\phi\omega_0^2\beta^{*2}}{\pi^2}$$

$$\left. \times \left\{ \frac{\omega_0\pi^2 4}{4\sqrt{x_2}\beta^*} \cos \left[\left(\pi - \frac{4\pi\tau_0^*\omega_0}{\beta^*} \right) \frac{\sqrt{x_2}2\beta^*}{\omega_0\pi} \right] \right\} \right.$$

$$\left. \times \operatorname{cosec} \frac{2\sqrt{x_2}\beta^*}{\omega_0} + \frac{\omega_0\pi^2}{8x_{20}\beta^{*2}} \right\} + \frac{4\Delta\omega_0^2\beta^{*2}}{\pi^2}$$

$$\left. \times \left\{ \frac{\omega_0\pi^2 4}{4\sqrt{x_3}\beta^*} \cos \left[\left(\pi - \frac{4\pi\tau_0^*\omega_0}{\beta^*} \right) \frac{\sqrt{x_3}2\beta^*}{\omega_0\pi} \right] \right\} \right.$$

$$\left. \times \operatorname{cosec} \frac{2\sqrt{x_3}\beta^*}{\omega_0} + \frac{\omega_0\pi^2}{8x_3\beta^{*2}} \right\} \left. \right\}.$$

On the other hand, for the non-oscillating transport mode the result has the form

$$S_B = 2(1+b)a\tau_0 - \frac{1}{2\beta}\omega_0^2(1+b)^2\tau_0^{*2} - \frac{4\omega_0^4(1+b)^2\{U_1 - U_2\}}{\beta},$$

where

$$\tau_0 = \frac{1}{2\omega_0} \operatorname{arcsinh} \left[\frac{b-a}{b+a} \sinh \frac{\omega_0\beta}{4} \right] + \frac{\beta}{4}$$

$$= \frac{1}{2\omega_0} \operatorname{arcsinh} \left[\frac{\frac{b-1}{a} \sinh \frac{\omega_0\beta}{4}}{\frac{b+1}{a}} \right] + \frac{\beta}{4},$$

or

$$\tau_0^* = \omega_0 \tau_0 = \frac{1}{2} \operatorname{arcsinh} \left[\frac{b^* - 1}{b^* + 1} \sinh \beta^* \right] + \beta^*.$$

If $x_1, x_2, x_3 < 0$ ($x_{10}, x_{20}, x_{30} > 0$), then:

$$U_1 = \frac{1}{2} \left\{ \beta_0 \frac{\beta^2}{24} + \frac{\gamma \beta^2}{4\pi^2} \left[\frac{1}{\tilde{x}_{10}^2} + \frac{\pi}{2\tilde{x}_{10}} \coth(\pi \tilde{x}_{10}) \right] \right. \\ \left. + \frac{\phi \beta^2}{4\pi^2} \left[\frac{1}{2\tilde{x}_{20}^2} + \frac{\pi}{2\tilde{x}_{20}} \coth(\pi \tilde{x}_{20}) \right] \right. \\ \left. + \frac{\Delta \beta^2}{4\pi^2} \left[\frac{1}{2\tilde{x}_{30}^2} + \frac{\pi}{2\tilde{x}_{30}} \coth(\pi \tilde{x}_{30}) \right] \right\},$$

$$U_2 = \frac{1}{2} \left\{ \frac{\beta_0 \beta^2}{48} \left(3 \left(\frac{4\pi \tau_0}{\beta} \right)^2 - \frac{24\pi^2 \tau_0}{\beta} + 2\pi^2 \right) \right. \\ \left. + \frac{\gamma \beta^2}{4\pi^2} \left\{ \frac{\pi^2}{\sqrt{x_{10}} \beta} \cosh \left[\left(\pi - \frac{4\pi \tau_0}{\beta} \right) \frac{\sqrt{x_{10}} \beta}{2\pi} \right] \right. \right. \\ \left. \left. \times \operatorname{cosech} \frac{\sqrt{x_{10}} \beta}{2} - \frac{2\pi^2}{x_{10} \beta^2} \right\} \right. \\ \left. + \frac{\phi \beta^2}{4\pi^2} \left\{ \frac{\pi^2}{\sqrt{x_{20}} \beta} \cosh \left[\left(\pi - \frac{4\pi \tau_0}{\beta} \right) \frac{\sqrt{x_{20}} \beta}{2\pi} \right] \right. \right. \\ \left. \left. \times \operatorname{cosech} \frac{\sqrt{x_{20}} \beta}{2} - \frac{2\pi^2}{x_{20} \beta^2} \right\} \right. \\ \left. + \frac{\Delta \beta^2}{4\pi^2} \left\{ \frac{\pi^2}{\sqrt{x_{30}} \beta} \cosh \left[\left(\pi - \frac{4\pi \tau_0}{\beta} \right) \frac{\sqrt{x_{30}} \beta}{2\pi} \right] \right. \right. \\ \left. \left. \times \operatorname{cosech} \frac{\sqrt{x_{30}} \beta}{2} - \frac{2\pi^2}{x_{30} \beta^2} \right\} \right\}.$$

Now we calculate the preexponential factor B with allowance for two promoting phonon modes

$$B = \frac{2\omega_0^2(a+b)}{(2\pi\beta)^{\frac{1}{2}}} \frac{\sum_{n=-\infty}^{\infty} \frac{\sin^2 \nu_n \tau_0}{\lambda_{0n}}}{\left[\sum_{n=-\infty}^{\infty} \frac{\cos 2\nu_n \tau_0}{\lambda_{0n}} \right]^{\frac{1}{2}}},$$

where $\lambda_{0n} = \nu_n^2 + \omega_0^2 + \zeta_n$.

The dimensionless preexponential factor is determined by the sums of two types

$$\tilde{B} = \frac{B}{a^2 \omega^{\frac{3}{2}}} = \frac{2\omega_0^2 \left(\frac{b}{a} + 1 \right)^2}{(2\pi\beta)^{\frac{1}{2}}} \frac{V_1}{(V_2)^{\frac{1}{2}}}, \\ V_1 = \sum_{n=-\infty}^{\infty} \frac{\sin^2 \nu_n \tau_0}{\lambda_{0n}} \\ = \frac{1}{2} \frac{D\beta^2}{4\pi^2} \left[-\frac{4\pi^2}{x_1 \beta^2} + 2 \left\{ -\frac{2\pi^2}{x_{10} \beta^2} - \frac{\pi^2}{\sqrt{x_1} \beta} \cot \frac{\sqrt{x_1} \beta}{2} \right\} \right] \\ + \frac{1}{2} \frac{E\beta^2}{4\pi^2} \left[-\frac{4\pi^2}{x_2 \beta^2} + 2 \left\{ -\frac{2\pi^2}{x_{20} \beta^2} - \frac{\pi^2}{\sqrt{x_2} \beta} \cot \frac{\sqrt{x_2} \beta}{2} \right\} \right] \\ + \frac{1}{2} \frac{F\beta^2}{4\pi^2} \left[-\frac{4\pi^2}{x_3 \beta^2} + 2 \left\{ -\frac{2\pi^2}{x_{30} \beta^2} - \frac{\pi^2}{\sqrt{x_3} \beta} \cot \frac{\sqrt{x_3} \beta}{2} \right\} \right] \\ - \frac{1}{2} \frac{D\beta^2}{4\pi^2} \left[-\frac{4\pi^2}{x_1 \beta^2} + 2 \left\{ -\frac{\pi^2}{\sqrt{x_1} \beta^2} \cos \left[\left(\pi - \frac{4\pi \tau_0}{\beta} \right) \frac{\sqrt{x_1} \beta}{2\pi} \right] \right. \right. \\ \left. \left. \times \operatorname{cosec} \frac{\sqrt{x_1} \beta}{2} + \frac{2\pi^2}{x_1 \beta^2} \right\} \right] \\ - \frac{1}{2} \frac{E\beta^2}{4\pi^2} \left[-\frac{4\pi^2}{x_2 \beta^2} + 2 \left\{ -\frac{\pi^2}{\sqrt{x_2} \beta^2} \cos \left[\left(\pi - \frac{4\pi \tau_0}{\beta} \right) \frac{\sqrt{x_2} \beta}{2\pi} \right] \right. \right. \\ \left. \left. \times \operatorname{cosec} \frac{\sqrt{x_2} \beta}{2} + \frac{2\pi^2}{x_2 \beta^2} \right\} \right] \quad (A6) \\ - \frac{1}{2} \frac{F\beta^2}{4\pi^2} \left[-\frac{4\pi^2}{x_3 \beta^2} + 2 \left\{ -\frac{\pi^2}{\sqrt{x_3} \beta^2} \cos \left[\left(\pi - \frac{4\pi \tau_0}{\beta} \right) \frac{\sqrt{x_3} \beta}{2\pi} \right] \right. \right. \\ \left. \left. \times \operatorname{cosec} \frac{\sqrt{x_3} \beta}{2} + \frac{2\pi^2}{x_3 \beta^2} \right\} \right], \\ V_2 = \sum_{n=-\infty}^{\infty} \frac{\cos 2\nu_n \tau_0}{\lambda_{0n}} \\ = \frac{D\beta^2}{4\pi^2} \left[-\frac{4\pi^2}{x_1 \beta^2} + 2 \left\{ -\frac{\pi^2}{\sqrt{x_1} \beta^2} \cos \left[\left(\pi - \frac{4\pi \tau_0}{\beta} \right) \frac{\sqrt{x_1} \beta}{2\pi} \right] \right. \right. \\ \left. \left. \times \operatorname{cosec} \frac{\sqrt{x_1} \beta}{2} + \frac{2\pi^2}{x_1 \beta^2} \right\} \right]$$

$$\begin{aligned}
 & + \frac{E\beta^2}{4\pi^2} \left[-\frac{4\pi^2}{x_2\beta^2} + 2 \left\{ -\frac{\pi^2}{\sqrt{x_2}\beta^2} \cos \left[\left(\pi - \frac{4\pi\tau_0}{\beta} \right) \frac{\sqrt{x_2}\beta}{2\pi} \right] \right. \right. \\
 & \quad \left. \left. \times \operatorname{cosech} \frac{\sqrt{x_2}\beta}{2} - \frac{2\pi^2}{x_2\beta^2} \right\} \right], \\
 & \quad \times \operatorname{cosec} \frac{\sqrt{x_2}\beta}{2} + \frac{2\pi^2}{x_2\beta^2} \left. \right\} \\
 & + \frac{F\beta^2}{4\pi^2} \left[-\frac{4\pi^2}{x_3\beta^2} + 2 \left\{ -\frac{\pi^2}{\sqrt{x_3}\beta^2} \cos \left[\left(\pi - \frac{4\pi\tau_0}{\beta} \right) \frac{\sqrt{x_3}\beta}{2\pi} \right] \right. \right. \\
 & \quad \left. \left. \times \operatorname{cosec} \frac{\sqrt{x_3}\beta}{2} + \frac{2\pi^2}{x_3\beta^2} \right\} \right], \\
 & \quad \times \operatorname{cosec} \frac{\sqrt{x_3}\beta}{2} + \frac{2\pi^2}{x_3\beta^2} \left. \right\}, \\
 & \quad V_2 = \sum_{n=-\infty}^{\infty} \frac{\cos 2v_n\tau_0}{\lambda_{0n}} \\
 & = \frac{1}{2} \frac{D\beta^2}{4\pi^2} \left[-\frac{4\pi^2}{x_1\beta^2} + \left\{ \frac{\pi^2}{x_{10}\beta^2} + \frac{\pi^2}{\sqrt{x_{10}}\beta^2} \right. \right. \\
 & \quad \left. \left. \times \cosh \left[\left(1 - \frac{4\tau_0}{\beta} \right) \frac{\sqrt{x_{10}}\beta}{2} \right] \operatorname{cosech} \frac{\sqrt{x_{10}}\beta}{2} - \frac{2\pi^2}{x_{10}\beta^2} \right\} \right] \\
 & - \frac{1}{2} \frac{E\beta^2}{4\pi^2} \left[-\frac{4\pi^2}{x_2\beta^2} + 2 \left\{ \frac{\pi^2}{x_{20}\beta^2} + \frac{\pi^2}{\sqrt{x_{20}}\beta^2} \coth \frac{\sqrt{x_{20}}\beta}{2} \right\} \right] \\
 & - \frac{1}{2} \frac{F\beta^2}{4\pi^2} \left[-\frac{4\pi^2}{x_3\beta^2} + 2 \left\{ \frac{\pi^2}{x_{30}\beta^2} + \frac{\pi^2}{\sqrt{x_{30}}\beta^2} \coth \frac{\sqrt{x_{30}}\beta}{2} \right\} \right].
 \end{aligned}$$

For the non-oscillating transport mode the result takes the form

$$\tilde{B} = \frac{B}{a^2 \omega^{3/2}} = \frac{2(b^* + 1)^2}{(2\pi\beta^*)^{1/2}} \frac{\tilde{V}_1}{(\tilde{V}_2)^{1/2}},$$

$$V_1 = \sum_{n=-\infty}^{\infty} \frac{\sin^2 v_n \tau_0}{\lambda_{0n}}$$

$$\begin{aligned}
 & = \frac{1}{2} \frac{D\beta^2}{4\pi^2} \left[-\frac{4\pi^2}{x_1\beta^2} + 2 \left\{ \frac{2\pi^2}{x_{10}\beta^2} + \frac{\pi^2}{\sqrt{x_{10}}\beta} \coth \frac{\sqrt{x_{10}}\beta}{2} \right\} \right] \\
 & + \frac{1}{2} \frac{E\beta^2}{4\pi^2} \left[-\frac{4\pi^2}{x_2\beta^2} + 2 \left\{ \frac{2\pi^2}{x_{20}\beta^2} + \frac{\pi^2}{\sqrt{x_{20}}\beta} \coth \frac{\sqrt{x_{20}}\beta}{2} \right\} \right] \\
 & + \frac{1}{2} \frac{F\beta^2}{4\pi^2} \left[-\frac{4\pi^2}{x_3\beta^2} + 2 \left\{ \frac{2\pi^2}{x_{30}\beta^2} + \frac{\pi^2}{\sqrt{x_{30}}\beta} \coth \frac{\sqrt{x_{30}}\beta}{2} \right\} \right] \\
 & - \frac{1}{2} \frac{D\beta^2}{4\pi^2} \left[-\frac{4\pi^2}{x_1\beta^2} + 2 \left\{ \frac{\pi^2}{\sqrt{x_{10}}\beta^2} \cosh \left[\left(1 - \frac{4\tau_0}{\beta} \right) \frac{\sqrt{x_{10}}\beta}{2} \right] \right. \right. \\
 & \quad \left. \left. \times \operatorname{cosech} \frac{x_{10}\beta}{2} - \frac{2\pi^2}{x_{10}\beta^2} \right\} \right] \\
 & - \frac{1}{2} \frac{E\beta^2}{4\pi^2} \left[-\frac{4\pi^2}{x_2\beta^2} + 2 \left\{ \frac{\pi^2}{\sqrt{x_{20}}\beta^2} \cosh \left[\left(1 - \frac{4\tau_0^*}{\beta^*} \right) \frac{\sqrt{x_{20}}\beta}{2} \right] \right. \right. \\
 & \quad \left. \left. \times \operatorname{cosech} \frac{\sqrt{x_{20}}\beta}{2} - \frac{2\pi^2}{x_{20}\beta^2} \right\} \right] \\
 & - \frac{1}{2} \frac{F\beta^2}{4\pi^2} \left[-\frac{4\pi^2}{x_3\beta^2} + 2 \left\{ \frac{\pi^2}{\sqrt{x_{30}}\beta^2} \cosh \left[\left(1 - \frac{4\tau_0}{\beta} \right) \frac{\sqrt{x_{30}}\beta}{2} \right] \right. \right. \\
 & \quad \left. \left. \times \operatorname{cosech} \frac{\sqrt{x_{30}}\beta}{2} - \frac{2\pi^2}{x_{30}\beta^2} \right\} \right]
 \end{aligned}$$

REFERENCES

1. Y. Imry, *Introduction to Mesoscopic Physics* (Oxford: Oxford Univ., 1997; Moscow, 2002).
2. A. O. Caldeira and A. J. Leggett, *Phys. Rev. Lett.* **46**, 211 (1981).
3. A. I. Larkin and Yu. N. Ovchinnikov, *Pis'ma Zh. Eksp. Teor. Fiz.* **37**, 322 (1983).
4. A. I. Larkin and Yu. N. Ovchinnikov, *Zh. Eksp. Teor. Fiz.* **91**, 318 (1986).
5. V. F. Gantmakher and M. V. Feigel'man, *Phys.-Usp.* **41**, 105 (1998).
6. I. M. Ternov, V. Ch. Zhukovskii, and A. V. Borisov, *Quantum Mechanics and Mesoscopic Effects* (Moscow, 1993) [in Russian].
7. A. K. Aryngazin, V. Ch. Zhukovskii, V. D. Krevchik, A. A. Ovchinnikov, Yu. I. Dakhnovskii, M. B. Semenov, and A. I. Ternov, *Introduction in Contemporary Mesoscopics* (Penza: Penz. Gos. Univ., 2003) [in Russian].
8. K. Yamamoto, *Transfer Processes in Low-Dimensional Systems. Collection of Papers*, Ed. by A. K. Aryngazin, V. D. Krevchik, M. B. Semenov, and K. Yamamoto, (Tokyo: UT Res. Inst., 2005).
9. *Controlled Dissipative Tunneling. Tunnel Transport in Low-dimensional Systems*, Ed. by E. Legget, A. K. Aryngazin, M. B. Semenov, V. D. Krevchik, Yu. N. Ovchinnikov, and K. Yamamoto, (Moscow, 2011) [in Russian].
10. P. A. Borodin, A. A. Bukharaev, D. O. Filatov, D. A. Vorontsov, and M. A. Lapshina, *J. Surf. Invest.: X-ray, Synchron., Neutron Tech.* **3**, 721 (2009).
11. V. D. Krevchik, M. B. Semenov, R. V. Zaitsev, S. E. Kozenko, and M. A. Manukhina, *Izv. Vyssh. Ucheb. Zaved. Povolzh. Region. Fiz.-Mat. Nauki*, No. 2, 119 (2012).
12. Yu. I. Dakhnovskii, A. A. Ovchinnikov, and M. B. Semenov, *JETP* **65**, 541 (1987).

13. A. K. Aringazin, Yu. I. Dahnovsky, V. D. Krevchik, M. B. Semenov, V. A. Veremyev, A. A. Ovchinnikov, and K. Yamamoto, *Hadronic J.* **27**, 115 (2004).
14. A. Venkatesan, K. J. Lulla, M. J. Patton, A. D. Armour, C. J. Mellor, and J. R. Owers-Bradley J.R., (Nottingham: School of Physics and Astron., Univ. of Nottingham, NG72RD, arXiv:0912.1281v1 [cond-mat.meshall], (2009).
15. Yu. Bomze, H. Mebrahtu, I. Borzenets, A. Makarovski, and G. Finkelstein, G., (Durham: Department of Physics, Duke Univ., NC27708, arXiv:1010.1527v1 [cond-mat.meshall], (2010).
16. D. K. Ferry, S. M. Goodnick, and J. Bird. <http://www.cambridge.org/9780521877480>
17. L. G. D. da Silva and E. Dagotto, *Phys. Rev. B: Condens. Matter Mater. Phys.* **79**, 155302 (2009).
18. A. Grodecka, P. Machnikowski, and J. Forstner, arXiv: 0803., 1734v2 [cond-mat.mehall], (2009).
19. B. Ch. Zhukovskii, Yu. I. Dakhnovskii, O. N. Gorshkov, V. D. Krevchik, M. B. Semenov, Yu. G. Smirnov, E. V. Chuprunov, V. A. Rudin, N. Yu. Skibitskaya, P. V. Krevchik, D. O. Filatov, D. A. Antonov, M. A. Lashina, K. Yamamoto, and M. E. Shenina, *Mos. Univ. Phys. Bull.* **64**, 475 (2009).
20. B. Ch. Zhukovskii, Yu. I. Dakhnovskii, V. D. Krevchik, M. B. Semenov, V. G. Maiorov, E. I. Kudryashov, and K. Yamamoto, *Mos. Univ. Phys. Bull.*, No. 3, 24 (2006).
21. V. Ch. Zhukovskii, O. N. Gorshkov, V. D. Krevchik, M. B. Semenov, D. O. Filatov, D. A. Antonov, and E. V. Groznaya, *Mos. Univ. Phys. Bull.* **64**, 27 (2009).
22. V. Ch. Zhukovskii, Yu. I. Dakhnovskii, V. D. Krevchik, M. B. Semenov, V. G. Maiorov, E. I. Kudryashov, E. V. Shcherbakova, and K. Yamamoto, *Mos. Univ. Phys. Bull.* **62**, 73 (2007).
23. D. Filatov, V. Shengurov, N. Nurgazizov, et al., Tunneling atomic force microscopy of self-assembled In(Ga)As/GaAs quantum dots and rings and of GeSi/Si(001) nanoislands, in *Fingerprints in the Optical and Transport Properties of Quantum Dots*, Ed. by A. Al-Ahmadi, (Rijeka: InTech, 2012), p. 273.
24. A. Bolz, C. Meyer, T. Maltezopoulos, C. Heyn, W. Hansen, M. Morgenstern, and R. Wiesendanger, *Phys. Rev. Lett.* **91**, 196804 (2003).
25. A. A. Bukharaev, N. V. Berdunov, D. V. Ovchinnikov, and K. M. Salikhov, *Russ. Microelectr.* **26**, 137 (1997).

Translated by G. Dedkov